Organic & Biomolecular Chemistry

PAPER

View Article Online
View Journal

Cite this: DOI: 10.1039/c4ob02526a

An asymmetric pericyclic cascade approach to 3-alkyl-3-aryloxindoles: generality, applications and mechanistic investigations†

Edward Richmond,[a] Kenneth B. Ling,[a] Nicolas Duguet,[a] Lois B. Manton,[a] Nihan Çelebi-Ölçüm,[b,c] Yu-Hong Lam,[b] Sezen Alsancak,[c] Alexandra M. Z. Slawin,[a] K. N. Houk*[b] and Andrew D. Smith*[a]

Received 2nd December 2014,
Accepted 3rd December 2014

DOI: 10.1039/c4ob02526a

www.rsc.org/obc

The reaction of L-serine derived *N*-arylnitrones with alkylarylketenes generates asymmetric 3-alkyl-3-aryl-oxindoles in good to excellent yields (up to 93%) and excellent enantioselectivity (up to 98% ee) *via* a pericyclic cascade process. The optimization, scope and applications of this transformation are reported, alongside further synthetic and computational investigations. The preparation of the enantiomer of a Roche anti-cancer agent (RO4999200) **1** (96% ee) in three steps demonstrates the potential utility of this methodology.

Introduction

Cascade reactions are highly desirable owing to the ability to perform multiple sequential transformations without the necessity for additional manipulation or introduction of further reagents. Such approaches allow significant molecular complexity to be rapidly assembled, provided each subsequent transformation in the cascade unmasks a desirable, reactive functionality.[1] Pericyclic cascades are particularly attractive given their predictable regio- and stereocontrol,[2] coupled with the potential to readily generate multiple carbon–carbon bonds. Significant attention has focused on the expansion of this field toward both carbocyclic and heterocyclic frameworks.[3] The 3,3-disubstituted oxindole scaffold is an appealing target given the prevalence of naturally occurring species[4] and medicinal agents containing this core structure.[5] Notably, alkaloids **2**[6] and **3**[7] have both been prepared from 3,3-disubstituted oxindole precursors (Fig. 1).

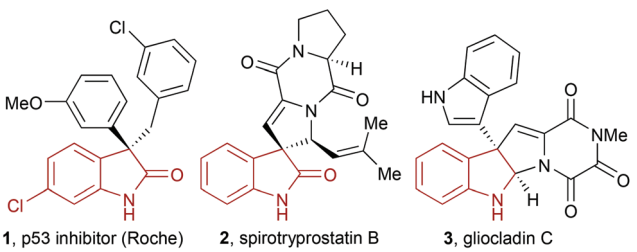

Fig. 1 Oxindole medicinal agent **1** and natural products **2** and **3** accessed synthetically from 3,3-disubstituted oxindoles.

As a consequence of their wide-ranging biological properties, and given the synthetic community's interest in developing novel approaches toward the preparation of molecules with quaternary stereocentres,[8] 3,3-disubstituted oxindoles have emerged as ideal frameworks on which to develop new asymmetric methodologies.[9] Typically, such approaches employ anilides, isatins or suitably substituted oxindole derivatives as starting materials (Fig. 2), although numerous other standalone approaches have also been developed.[9b,c,10–12] Asymmetric intramolecular anilide cyclizations[13] or Heck reactions[14] typically employ a palladium catalyst in combination with chiral ligands (a), and have found wide application in synthesis.[15] In similar systems, direct coupling approaches, without the necessity for pre-activation have been developed.[16] However, these approaches have yet to be rendered enantioselective. *O*-to-*C* transfer reactions (b) have also been used to great effect including Trost's asymmetric allylic alkylation methodology,[17] and Lewis base-catalyzed *O*-to-*C* carboxyl transfer reactions.[18] A plethora of catalytic

[a]*EaStCHEM, School of Chemistry, University of St Andrews, North Haugh, St Andrews KY16 9ST, UK. E-mail: ads10@st-andrews.ac.uk*
[b]*Department of Chemistry and Biochemistry, University of California, Los Angeles, 607 Charles E. Young Drive East, Los Angeles, CA 90095, USA. E-mail: houk@chem.ucla.edu*
[c]*Department of Chemical Engineering, Yeditepe University, Istanbul, 34755, Turkey*

†Electronic supplementary information (ESI) available: All spectroscopic data and procedures for novel compounds, computational methodology, comparision of B3LYP and MP2 geometries, full analysis of enantiomeric distributions, B3LYP-D geometries and energies, distortion–interaction analysis, the Cartesian coordinates of optimized structures, and the absolute energies and computed corrections of the reported geometries. CCDC 1029035–1029037. For ESI and crystallographic data in CIF or other electronic format see DOI: 10.1039/c4ob02526a

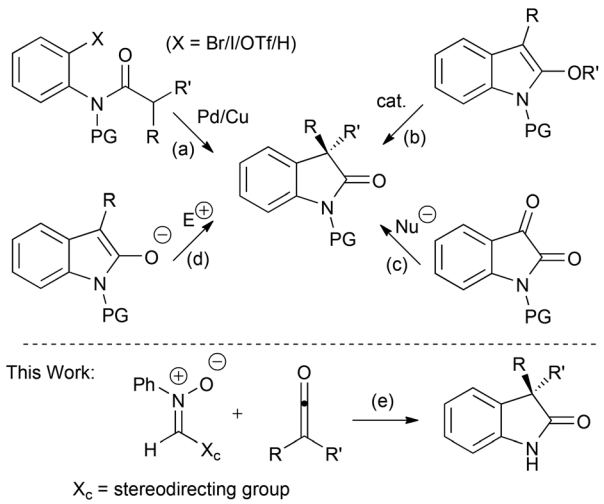

Fig. 2 Typical approaches toward asymmetric 3,3-disubstituted oxindoles.

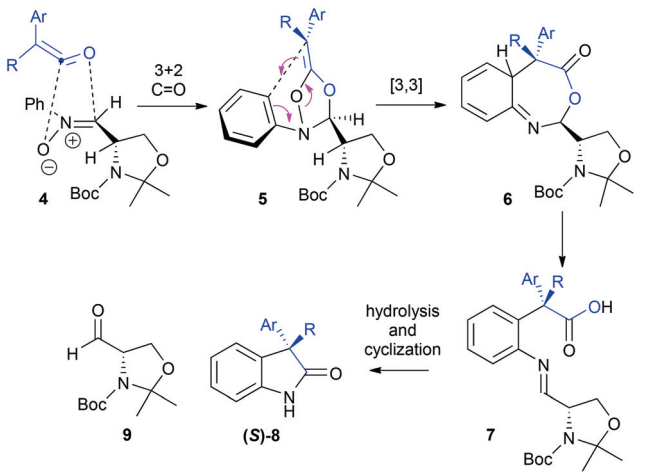

Fig. 3 Proposed mechanism.

methodologies has been developed over the past decade employing isatins (c) as starting materials,[19] giving access to 3-substituted-3-hydroxyoxindoles that serve as convenient synthetic intermediates.[20] Latterly, both stoichiometric and catalytic asymmetric alkylation approaches (d) have been reported to access 3,3-disubstituted oxindole species.[21] This manuscript details the asymmetric cycloaddition cascade reaction between nitrones and ketenes (e), allowing direct access to the unprotected 3,3-disubstituted oxindole motif. This method contrasts the commonly employed approaches that require protection of the amide functionality, thereby generating *N*-protected oxindoles.

Previous studies and mechanism

The hetero-Claisen approach to oxindoles using *N*-phenylnitrones and diphenylketene was first reported by Staudinger[22] and subsequently investigated by Lippman[23] and Taylor.[24] Despite its synthetic potential, an asymmetric variant of this process was overlooked until we developed an asymmetric route to 3,3-disubstituted oxindoles (up to 90% ee) using Garner's aldehyde derived *N*-aryl nitrones and disubstituted ketenes.[25] Subsequent studies extended this methodology to the construction of asymmetric 3,3-spirocarbocyclic oxindoles,[26] and computational studies led to a revised mechanistic rationale for these processes.[27] The mechanistic pathway is consistent with a 3 + 2 cycloaddition across the ketene C=O bond, with preferential *anti*-addition with respect to the aryl portion of the ketene. Facial selectivity in this cycloaddition is controlled by the preferred arrangement of large and electronegative allylic groups, and 1,3-allylic strain[28] within the enantiopure nitrone chiral auxiliary **4**, generating a stereodefined five-membered intermediate **5**. Subsequent [3,3]-sigmatropic rearrangement yields **6**, which undergoes rearomatization and tautomerization to give imino acid **7**. Each of these steps was established by computational studies of the reaction transition states.[27] Acidic hydrolysis and concomitant cyclization generate the oxindole **8** with excellent enantiocontrol and regenerate chiral aldehyde **9** (Fig. 3).[29]

The ability of this methodology to generate highly substituted quaternary stereocentres at the oxindole C(3)-position with excellent enantiocontrol (up to 90% ee), coupled with the low cost of the starting materials, warranted further development of this reaction manifold. To this end, this manuscript describes our studies devoted to the optimization of the levels of enantioselectivity in this transformation, alongside computational and experimental mechanistic studies of this process. The full scope and limitations of the optimized process are delineated, as well as its application to a target Roche anticancer agent (RO4999200).

Results and discussion

Stereodirecting group optimization

To explore the necessary structural requirements for generating high enantiocontrol in this reaction manifold, a range of enantiopure *N*-aryl nitrones **11–16** was synthesized from readily available chiral starting materials. These nitrones were then evaluated in the pericyclic cascade process with ethylphenylketene (Fig. 4).[30] Initially, Naproxen-derived nitrone **11** was synthesized and evaluated, generating oxindole **10** in a poor 27% ee. Mannitol-derived nitrone **12** proved more successful, providing oxindole **10** in 78% yield and 70% ee after treatment with ethylphenylketene. An α-oxygenated series of nitrones **13–16**, derived from (*S*)-ethyl lactate, was also synthesized and tested. These nitrones proved difficult to isolate and were consequently prepared and evaluated *in situ*.[31] A general trend of increasing enantioselectivity with increasing substituent size was observed, with *O*-TIPS-substituted nitrone **15** delivering **10** in 80% ee.

Subsequent studies prepared and evaluated a series of chiral nitrones bearing a protected nitrogen atom at the α-position (Fig. 5). The acyclic, α-dibenzylamino nitrone **17** provided the oxindole in 70% ee, but in poor yield. The *N*-Boc nitrone **4**,

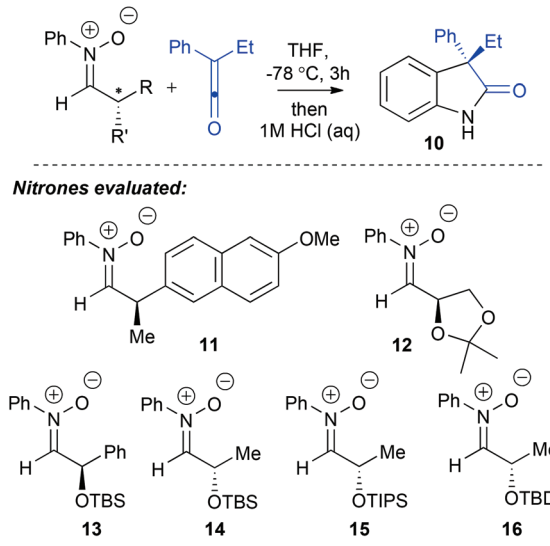

Entry	Nitrone	Oxindole Yield (%)[a]	Oxindole ee (%)[b]
1	**11**	43	27 (*ent*)
2	**12**	78	70 (*ent*)
3	**13**	25	< 5
4	**14**	32	60
5	**15**	70	80
6	**16**	38	32

Fig. 4 Variation of the chiral nitrone. [a]Isolated yield of oxindole **10** after purification by column chromatography. [b]Determined by chiral HPLC analysis.

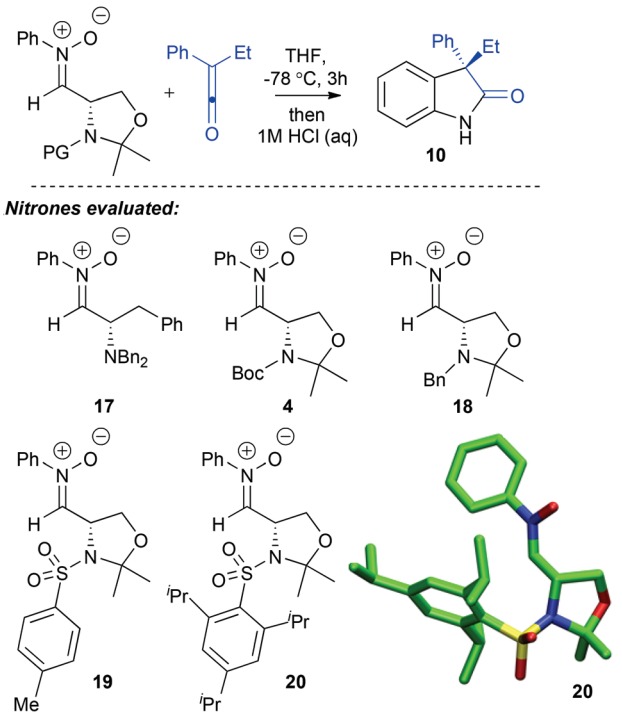

Entry	Nitrone	Oxindole Yield (%)[a]	Oxindole ee (%)[b]
1	**17**	21	70
2	**4**	83	84
3	**18**	60	20
4	**19**	75	91
5	**20**	86	96

Fig. 5 Optimization of stereodirecting groups on the nitrone and representation of the X-ray crystal structure of **20**. [a]Isolated yield of oxindole **10** after purification by column chromatography. [b]Determined by chiral HPLC analysis.

derived from Garner's aldehyde, gave oxindole **10** in good yield and 84% ee. This prompted us to evaluate a series of structural analogues of **4** in which the *N*-substituent is varied. Upon treatment with ethylphenylketene, the *N*-benzyl nitrone **18** gave the desired oxindole with poor enantiocontrol, suggesting that structural rigidity or restricted rotation at this position may be crucial to engendering high levels of enantioselectivity. As a consequence, a sulfonamide substituent was investigated. With *N*-tosyl nitrone **19**, the oxindole was obtained in good yield and excellent enantiocontrol (75% yield, 91% ee). Increasing the size of the sulfonamide group was found to improve the enantioselectivity, as the use of *N*-TIPBS (2,4,6-triisopropylbenzenesulfonyl) nitrone **20** furnished oxindole **10** in 86% yield and 96% ee. A single-crystal X-ray structure of **20** was obtained, and gives an excellent representation as to the steric impact of this TIPBS residue.[32] Further studies allowed for preparation of **20** on gram scale (see ESI† for details).

Computational studies – role of the *N*-substituent in determining enantioselectivity

In order to understand the origin of the effect of the size of the *N*-substituent on the enantioselectivity of the reaction, the competing stereoisomeric transition structures (TSs) for nitrones **4**, *ent*-**12**, and **20** were located using Gaussian 09[33] at the M06-2X/6-311+G(d,p)//B3LYP/6-31G(d) level. In the proposed mechanism, the stereochemical outcome of the reaction is determined at the 3 + 2 cycloaddition step of the pericyclic cascade simultaneously by the facial selectivity of the nitrone and the direction of attack on the ketene.[27] Our previous calculations have shown that the approach of ketene from the *Re* face of nitrone is strongly disfavored as it places the ring methylene group at the sterically more demanding inside position. Indeed, nitrones **4**, *ent*-**12** and **20** all displayed significantly high π-facial selectivities with the *Si* face attack contributing more than 97% to the diastereomeric cycloadduct distribution (see ESI†), and the competing stereodetermining factor was the orientation of the unsymmetrically substituted ketene at the TS (Fig. 6).

We initially considered the 2,2-dimethyl-1,3-dioxolanyl auxiliary (Fig. 6, X = O) to study the stereoinduction in the absence of steric interactions from the protecting group. The calculations predict a 1.4 kcal mol^{-1} difference in free energy between **TSE-O** and **TSZ-O** favoring the *trans* addition with respect to the phenyl portion of the ketene. The cycloaddition occurs in the plane of ketene substituents, and the observed *trans*-phenyl selectivity can be explained by the attack of nitrone from the least hindered side in the plane of ketene. Steric

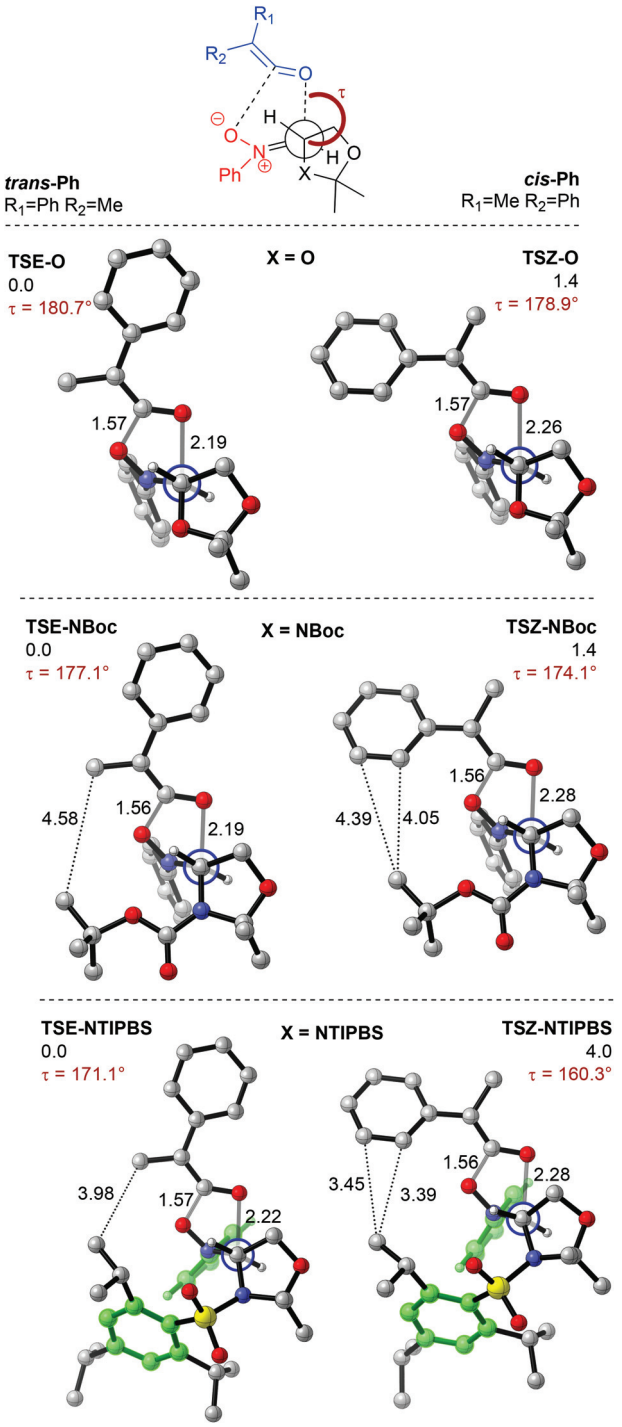

Fig. 6 Relative Gibbs free energies (in kcal mol^{-1}) of stereoselectivity-determining 3 + 2 cycloaddition transition structures for nitrones **4**, *ent*-**12** and **20**, calculated with M06-2X/6-311+G(d,p)(THF)//B3LYP/6-31G(d). The hydrogen atoms, except those around the Newman projections, are omitted for clarity.

effects of ketene substituents for nucleophilic additions at the ketene LUMO in the plane of substituents are well documented, and have been proposed to be responsible for high levels of *E*/*Z* selectivities obtained in the reactions of unsymmetrically substituted ketenes with carbon and oxygen nucleophiles.[34,35]

The inclusion of *N*-protected chiral auxiliaries leads to an increase in the *E*/*Z* selectivity by introducing a higher degree of steric hindrance at the transition structures with the Ph group *cis* (Fig. 6, X = NBoc and NTIPBS). While the additional contribution of *N*-PG to the selectivity is found to be minimal for *N*-Boc nitrone, the steric effects become significant with the increasing size of the protecting group, disfavoring **TSE-NTIPBS** compared with **TSZ-NTIPBS** with an energetic cost that amounts to 4.0 kcal mol^{-1}. Steric interactions between the *N*-substituent and the ketene substituents result in substantial deviations in the antiperiplanarity of the C–N bond at the TS. The O–C–C–N dihedral angle (τ) decreases with increasing size of the *N*-substituent and correlates well with the activation energy (R^2 = 0.94, see ESI†) suggesting a combination of steric and electronic effects in determining the selectivity of the reaction. A distortion-interaction analysis shows that both distortion and interaction energies favorably contribute to the stabilization of **TSE-NTIPBS** with respect to **TSZ-NTIPBS** (see ESI†). The edge-to-face π–π interaction displayed in the X-ray structure of nitrone **20** is well reproduced by the calculations (shown highlighted in Fig. 6).[36]

Scope and limitations

With *N*-TIPBS nitrone **20** established as the optimum chiral auxiliary for this asymmetric oxindole forming methodology, reactions with a range of alkylarylketenes were undertaken to demonstrate the scope and limitations of this transformation. To provide a direct comparison between the *N*-TIPBS and *N*-Boc nitrone chiral auxiliaries, the reactions with the same series of alkylarylketenes were selected, the results of which are summarized in Fig. 7. In all cases, an improvement in ee

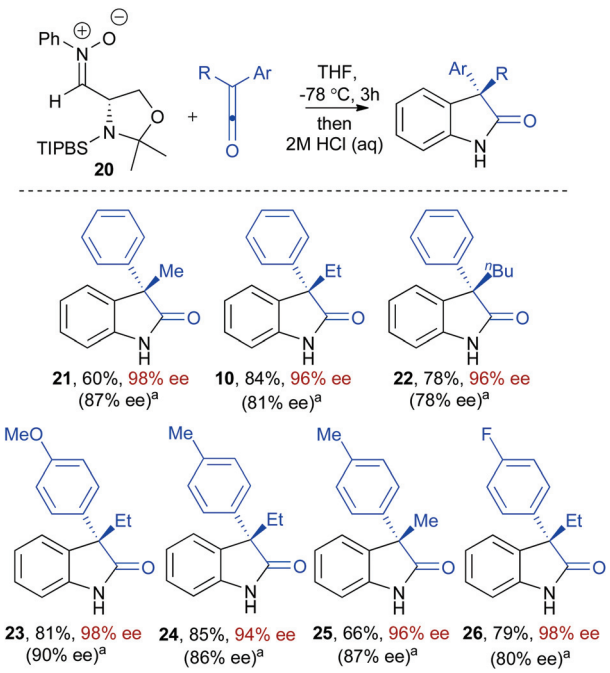

Fig. 7 Asymmetric oxindole synthesis using nitrone **20**; [a] ee values in parentheses represent those obtained using *N*-Boc nitrone **4**.[25]

was observed with *N*-TIPBS nitrone **20**, whilst yields remained high and a variety of aryl and alkyl substitution patterns at the C(3)-position of the oxindole were successfully incorporated (**21**–**26**).

Using the optimised *N*-TIBPS nitrone **20**, an extensive ketene screen showed that numerous alkylarylketenes were well tolerated in this process, yielding the respective oxindoles in good yields although varying ee (Fig. 8).[37] β-Branching of the alkyl group of the ketene component was well tolerated (**27**) and reaction with halo-arylketenes yielded oxindoles **28**, **29** and **30** in excellent ee. The transformation is also compatible with a C(3)-indolyl substituent, which is common to many natural products,[38] as oxindoles **31** and **32** were furnished in 88% and 84% ee, respectively. Ketenes bearing a 2-substituted phenyl ring (**33** and **34**) or a 1-naphthyl substituent (**35**) ring resulted in diminished enantiocontrol, yet these reactions still provided the desired oxindoles in moderate to excellent yields. α-Branching of the alkyl substituent resulted in a racemic mixture, as illustrated by the reaction generating oxindole **36**. Attempted extension to C(3)-tertiary asymmetric oxindoles using monosubstituted ketenes (generated *in situ*) allowed the isolation of oxindole **37** in a promising 72% yield and 50% ee. However, this species proved configurationally unstable, with slow racemization observed over time.[39] Oxindole **38** was generated using a solution of methylketene in 54% yield, but was racemic.

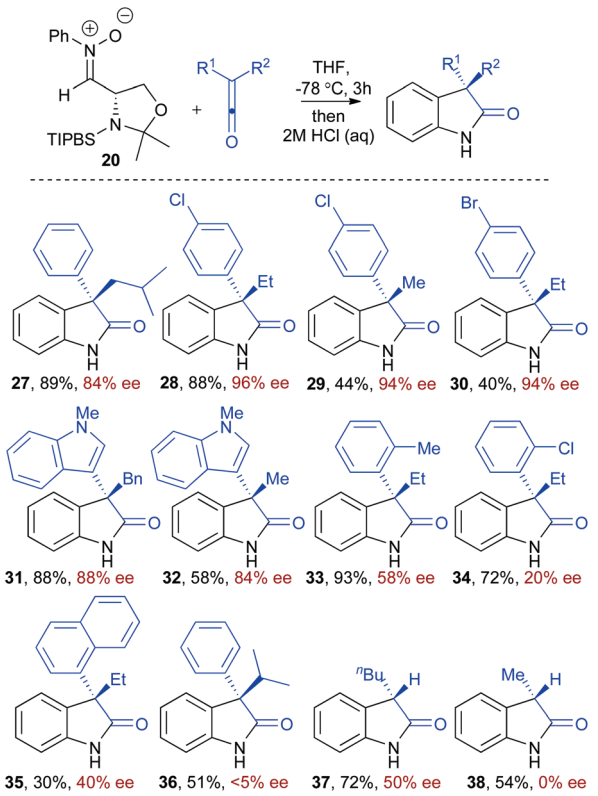

Fig. 8 Asymmetric oxindole synthesis; generality.

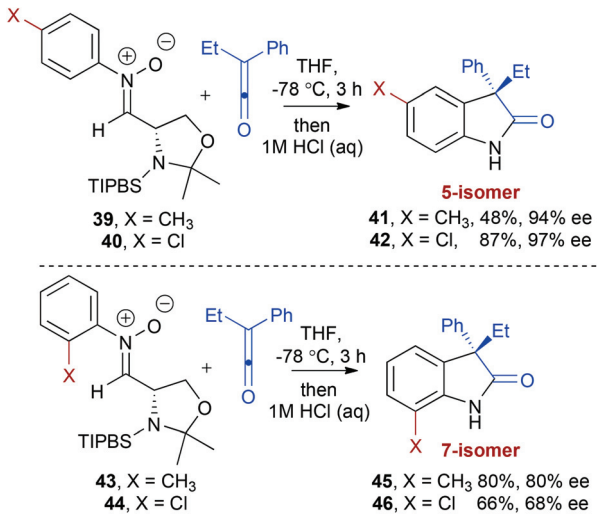

Fig. 9 Asymmetric oxindole synthesis using 4-(**39** and **40**) or 2-substituted (**43** and **44**) *N*-aryl nitrones.

Regioselectivity

Attention next turned to substitution of the *N*-aryl nitrone ring to probe the effect upon regio- and stereoselectivity of this process (Fig. 9). 4-Tolyl- and 4-chlorophenyl *N*-aryl nitrones **39** and **40** each gave the 5-substituted oxindole as a single regioisomer, in excellent ee and acceptable yields. Similarly, 2-tolyl nitrone **43** and 2-chlorophenyl nitrone **44** gave 7-substituted oxindoles **45** and **46**, respectively, as single regioisomers in good yield although with lower enantioselectivities.

However, treatment of 3-substituted *N*-aryl nitrones **47** and **48** (Fig. 10) with ethylphenylketene gave a 40 : 60 regioisomeric mixture of the 4- and 6-substituted oxindole isomers respectively, in good yields. Using 3-tolyl nitrone **47**, the ee of the inseparable 4- and 6-regioisomers was 91%, while 3-chlorophenyl nitrone **48** gave the separable 4- and 6-chlorooxindoles in 86% ee.

The computed regioselectivity-determining transition structures are shown in Fig. 11 for 3-tolyl nitrone **53** and methylphenylketene as the model reactants. According to the proposed pericyclic cascade mechanism, the regioselectivity is dictated by the hetero-Claisen rearrangement step of the 3 + 2

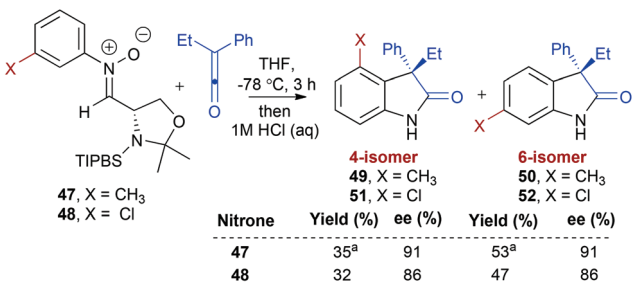

Nitrone	Yield (%)	ee (%)	Yield (%)	ee (%)
47	35[a]	91	53[a]	91
48	32	86	47	86

Fig. 10 Regioselectivity trends in the asymmetric oxindole synthesis using 3-substituted *N*-aryl nitrones. [a]oxindoles **49** and **50** were isolated and analyzed as a mixture of regioisomers in 88% combined yield: the reported yields refer to mol% fraction of total isolated material.

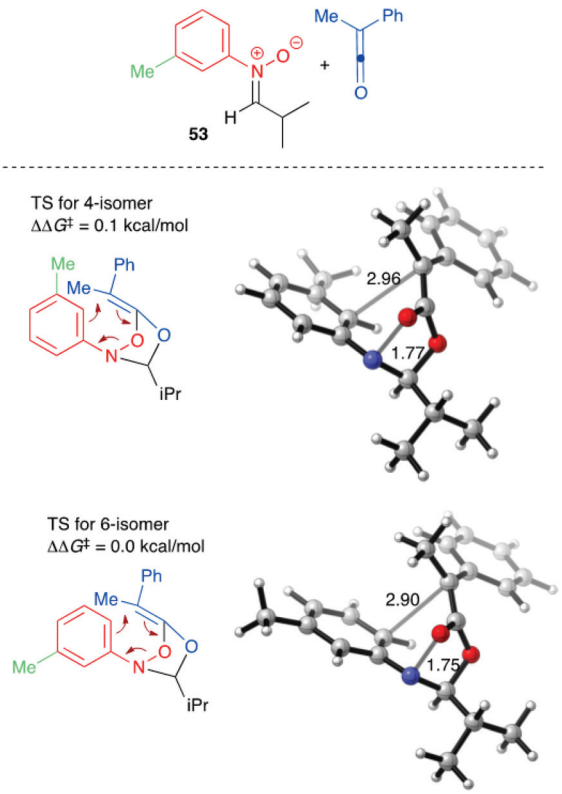

Fig. 11 Regioselectivity-determining transition structures (SCS-MP2/6-31G(d)(THF)//MP2/6-31G(d)(THF)) involving *meta*-substituted nitrones.

cycloadduct. This [3,3]-sigmatropic rearrangement is highly asynchronous since the C–C bond is barely formed when the N–O bond is being cleaved at the transition state. The perturbation by any substituent at either the 4- or the 6-position is therefore likely to be minimal. Indeed, the free energies of the transition structures for the 4-isomer and the 6-isomer were found to differ only by 0.1 kcal mol^{-1} in favor of the 6-isomer. This is essentially replicated in experimental investigations with ethylphenylketene (Fig. 10) where a minimal preference for the 6-isomer is observed in the case of both chloro- and methyl- substitution.

Mechanistic validation

In our recent communication, the computational exploration of the possible reaction pathways for the formation of the key imino acid intermediates in the reactions of *N*-phenyl nitrones with ketenes were evaluated at the M06-2X/6-311+G(d,p)//B3LYP/6-31G(d) level (Scheme 1).[27] These studies described a novel 1,3-dipolar cycloaddition and hetero-[3,3]-rearrangement cascade (Scheme 1, Pathway A) involving a chirality transfer between the highly asynchronous but concerted pericyclic steps. Here, we extend our calculations to the SCS-MP2/6-31G(d)//MP2/6-31G(d) level of theory (Fig. 12), which provided the best results in an equivalent key [3,3]-sigmatropic rearrangement step of the acid-promoted Fischer indole reaction, where B3LYP optimizations were shown to yield highly asynchronous and dissociative transition states.[40]

In the first step of the pericyclic cascade mechanism, the 3 + 2 cycloaddition between nitrone and ketene across the C=O bond forms the substituted 1,2,4-dioxazolidine. The 3 + 2 cycloaddition transition structure, **TS-(3 + 2)**, is predicted to be 16.7 kcal mol^{-1} uphill from the starting nitrone and ketene (Fig. 12). **TS-(3 + 2)** features two forming C–O bonds of 1.57 Å and 2.12 Å. The geometry and electronic features are in good agreement with the previously described 3 + 2 cycloaddition TS obtained using B3LYP.[27] This cycloaddition step sets the stereochemistry of the 5-membered ring in the cycloadduct involving an unsymmetrically substituted exocyclic alkylidene group. The cycloadduct **int-1** is 6.9 kcal mol^{-1} more stable relative to the separated reactants, and smoothly undergoes an aromatic hetero-[3,3]-sigmatropic shift *via* **TS-[3,3]** with an activation free energy of 2.3 kcal mol^{-1} furnishing the quaternary stereocenter. The subsequent stereospecific hetero-[3,3]-rearrangement step transfers the stereochemical information

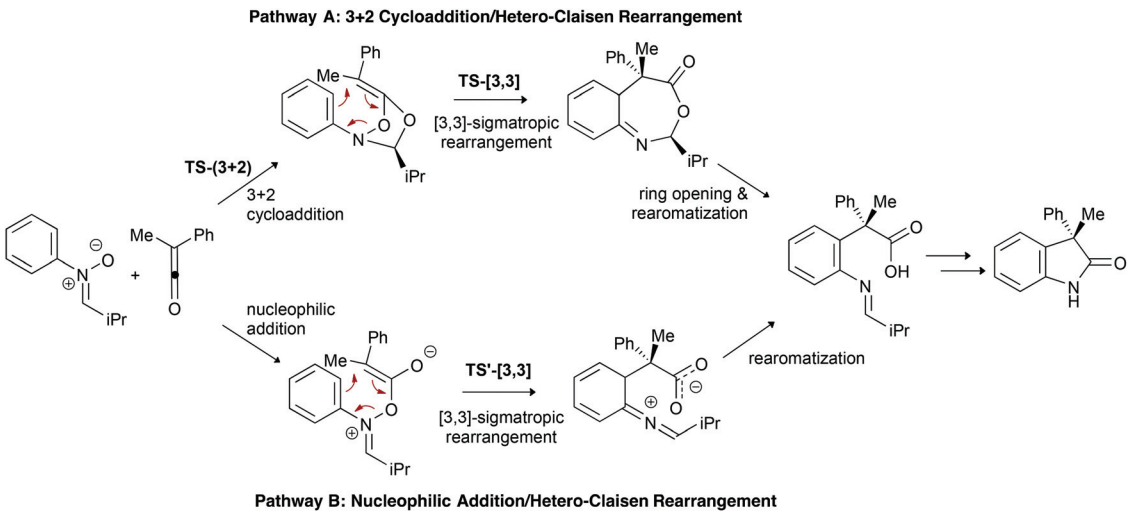

Scheme 1 Mechanistic proposals for the reactions of *N*-phenylnitrones with disubstituted ketenes.

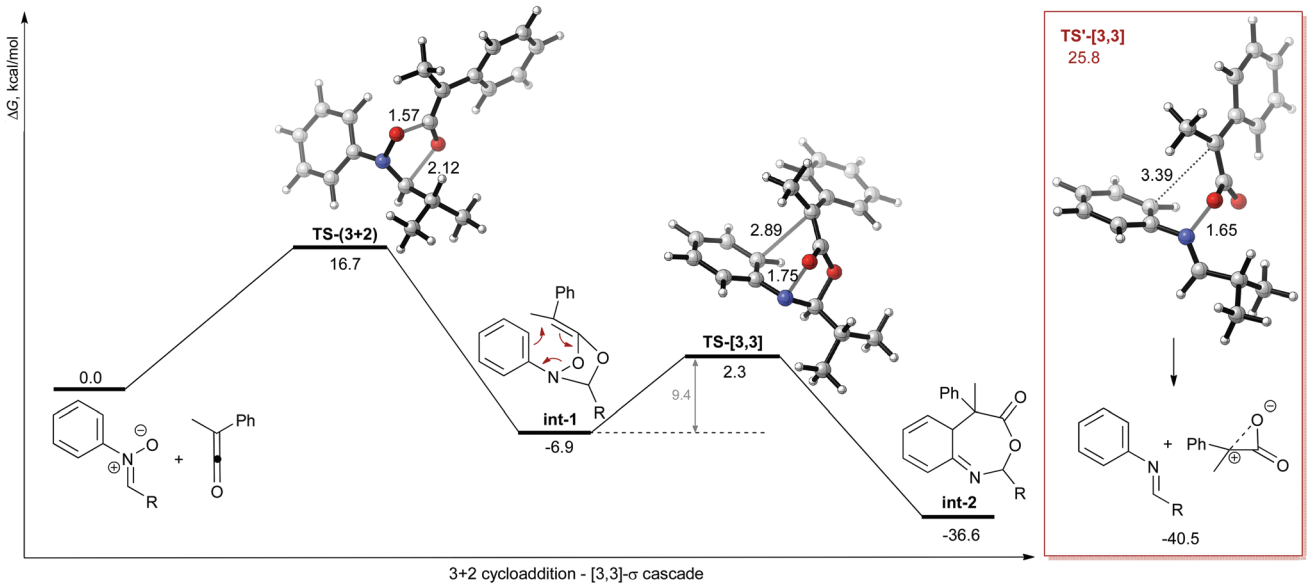

Fig. 12 Pericyclic cascade (Pathway A, Scheme 1) and competing heterolytic cleavage pathway (Pathway B, Scheme 1; **TS′-[3,3]**) (R = i-Pr). The relative free energies (Δ*G*, kcal/mol), calculated using SCS-MP2/6-31G(d)//MP2/6-31G(d), are given with respect to the separated reactants.

of the cycloadduct to intermediate **int-2**, installing the desired quaternary stereocenter. **TS-[3,3]** is early and highly asynchronous; the breaking N–O bond is 1.75 Å as the forming C–C bond is 2.89 Å. The critical distances in the MP2 optimized transition structure are significantly shorter compared with those predicted using B3LYP (d_{C-C}(B3LYP) = 3.47 Å, d_{N-O}(B3LYP) = 1.95 Å). The intrinsic reaction coordinate (IRC) path from **TS-[3,3]** indicates no intermediates, and connected the cycloadduct **int-1** to intermediate **int-2**, which has a relative free energy of −36.6 kcal mol^{-1} with respect to the separated reactants. Cleavage of the hemiaminal linkage and rearomatization form the aromatic imino acid.

An analogous [3,3]-rearrangement transition structure, **TS′-[3,3]**, in a previously proposed nucleophilic addition and hetero-Claisen rearrangement mechanism (Scheme 1, pathway B) led to dissociation rather than rearrangement (red inset, Fig. 12). This pathway has a higher free energy of activation ($\Delta G^{\ddagger}$ = 25.8 kcal mol^{-1}) than the pericyclic cascade ($\Delta G^{\ddagger}$ = 16.7 kcal mol^{-1}) and is, therefore, not observed experimentally.

Further mechanistic insight can be gleaned by comparing the sigmatropic rearrangement step in the acid-promoted Fischer indole reaction, the originally proposed, nucleophilic addition/hetero-Claisen rearrangement pathway (Pathway B, Scheme 1), and the pericyclic cascade pathway (Pathway A, Scheme 1). The key steps common to these three pathways are laid out in Fig. 13. The key step of the Fischer indole synthesis is an aromatic hetero-Claisen rearrangement (3,4-diaza-Cope rearrangement, Fig. 13a); this corresponds to a 3-aza,4-oxa-Cope rearrangement involved in both pathways A and B in the present study (Fig. 13b and c). Our previous work found that Fischer indolization substrates with certain substitution patterns, such as the one shown in Fig. 13a, do not undergo the

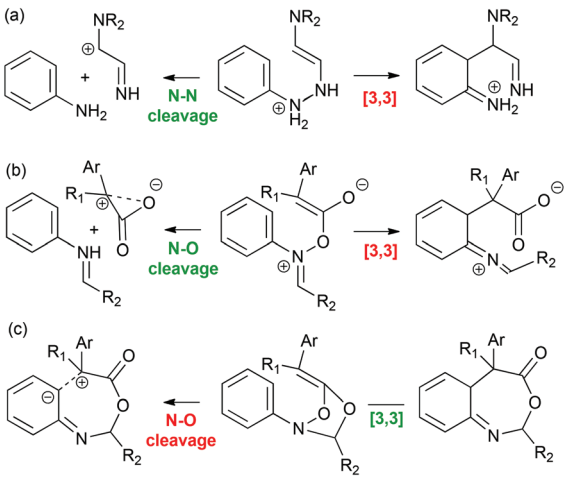

Fig. 13 Competing [3,3]-rearrangement and cleavage pathways (a) in the Fischer indole synthesis;[39] (b) in pathway B; (c) in pathway A.

desired rearrangement.[40] Instead, heterolysis of the N–N$^{(+)}$ bond occurs, giving an aniline and a resonance-stabilized carbocation. Our computations showed that these attempted rearrangements fail because the electron-donating groups on the terminal aliphatic carbon of the rearranging system significantly lower the bond dissociation enthalpy of the N–N$^{(+)}$ bond, and favor the heterolysis of this bond over the intended [3,3]-sigmatropic rearrangement. Similarly, 3-aza,4-oxa-Cope rearrangement transition states of pathways A and B contain a disubstituted alkylidene group derived from the ketene reactant (Fig. 13b and 13c). In accord with the previous findings,[40] the located transition structures, **TS-[3,3]** and **TS′-[3,3]** are both early and highly asynchronous, indicative of significant weakening of the O–N bond (Fig. 12). Our calculations predict that

TS-[3,3] in pathway A gives the rearranged product (Fig. 13c), but the analogous **TS′-[3,3]** in pathway B leads to heterolysis of the O–$N^{(+)}$ bond akin to the heterolytic cleavage of the N–$N^{(+)}$ bond in the Fischer indole reaction (Fig. 13b). The formation of the non-charge separated arylimine and α-lactone products (ΔG = −40.5 kcal mol^{-1}) favors heterolysis over rearrangement in pathway B. On the other hand, the ketene oxygen is involved in the hemiaminal linkage in the cycloadduct making the rearranging system in pathway A uncharged. With no formal positive charge on nitrogen, the subsequent [3,3]-shift proceeds *via* **TS-[3,3]** in a concerted manner. This rearrangement is facile, presumably driven by both the electronic effects that weaken the N–O bond and the release of the ring strain. Thus, the competing high-energy-barrier to heterolysis of the O–N^{+} bond disfavors the operation of the nucleophilic addition-hetero-Claisen pathway. By contrast, our proposed pathway proceeds first by a 3 + 2 cycloaddition, yielding an uncharged system, which can undergo facile [3,3]-rearrangement. Comparison of pathway B (Fig. 13b) and the case of a failed Fischer indolization attempt (Fig. 13a) suggests the importance of electronic effects in hetero-Claisen rearrangements.

Attempted intermediate isolation

Experimental validation of the computationally predicted cycloaddition pathway by trapping anticipated reaction intermediates was probed. Initially, in an attempt to preclude the proposed rearomatization step, *N*-xylyl nitrone **54** was prepared and treated with one equivalent of ethylphenylketene. However, rather than the expected seven-membered intermediate, dearomatized imino-lactone **55** was produced as a 3.5 : 1 mixture of diastereoisomers. The major diastereoisomer was isolated in 66% yield after crystallization from MeOH, with the relative configuration within **55** proven by X-ray crystallography (Scheme 2).[41]

Next, replacement of the nitrone *N*-aryl substituent with a saturated alkyl substituent, thereby removing the potential for

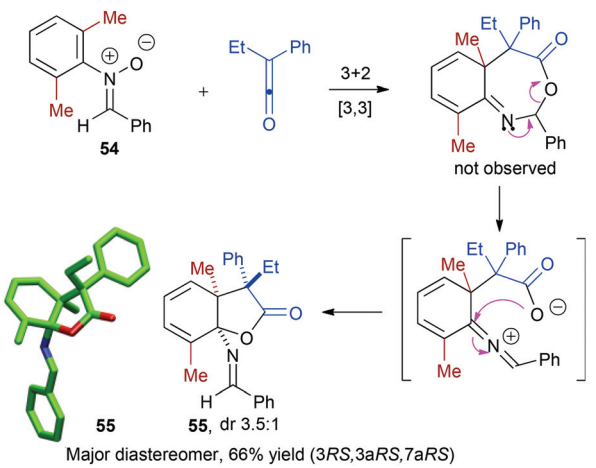

Major diastereomer, 66% yield (3*RS*,3a*RS*,7a*RS*)

Scheme 2 Formation of lactone **55** and representation of its X-ray crystal structure.

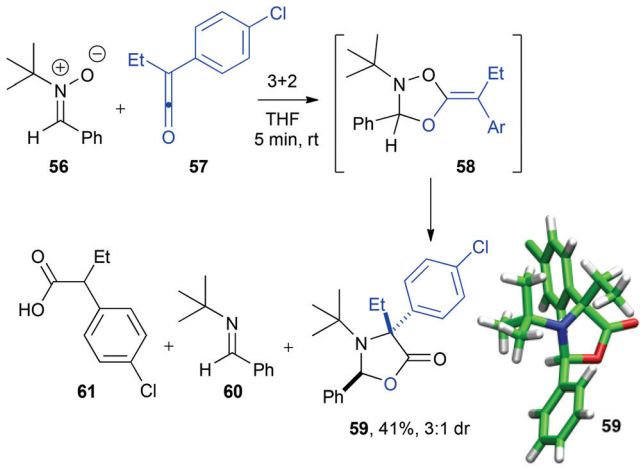

Scheme 3 Isolation of oxazolidinone **59** and representation of its X-ray crystal structure.

[3,3]-sigmatropic rearrangement, was investigated. Treatment of *N-tert*-butyl nitrone **56** with one equivalent of ethyl(*para*-chlorophenyl)ketene **57** gave oxazolidinone **59** in 3 : 1 crude dr (Scheme 3). The major diastereoisomer was isolated in 41% yield with *N-tert*-butyl imine also formed in this reaction.[42] Isolation of **59** provides indirect evidence for the computed reaction mechanism *via* initial 3 + 2 cycloaddition across the ketene C=O bond to furnish transient intermediate **58** which, *via* radical or ionic cleavage of the N–O bond, rearranges to generate the 5-membered oxazolidinone **59**.[43] An alternative dissociative decomposition of intermediate **58** can be envisaged to account for the generation of *N-tert*-butyl benzaldehyde imine **60** *via* N–O bond cleavage without concomitant C–C bond formation, resulting in elimination of the parent arylbutyric acid **61**.

Application to a target compound: anti-cancer agent

Finally, to demonstrate the efficiency of this pericyclic methodology and its potential utility in synthesis, Roche p53 inhibitor[44] (RO4999200) **1** was selected as a target, with *ent*-**1** synthesized in three simple steps from commercially available starting materials.[45] Recently, Kündig and co-workers reported the first asymmetric approach toward this species based upon a palladium-catalyzed intramolecular α-arylation,[46] while the Roche route relies upon chiral HPLC separation.[47] Feng and co-workers also recently reported an expedient catalytic preparation of **1**.[48] Our synthesis began with alkylation of commercially available *m*-anisylacetic acid **62**, followed by conversion to the acid chloride **63**, which was isolated in 87% yield over two steps. Dehydrohalogenation provided ketene **64**, which was used without isolation as a crude solution in THF (Scheme 4). In congruence with our regioselectivity studies, treatment of the *N*-3-chlorophenyl *N*′-TIPBS nitrone **48** with **64** provided a 60 : 40 mixture of 6- and 4-regioisomeric oxindoles, which could be readily separated by column chromatography over silica. Roche p53 inhibitor *ent*-**1** was isolated in 52% yield

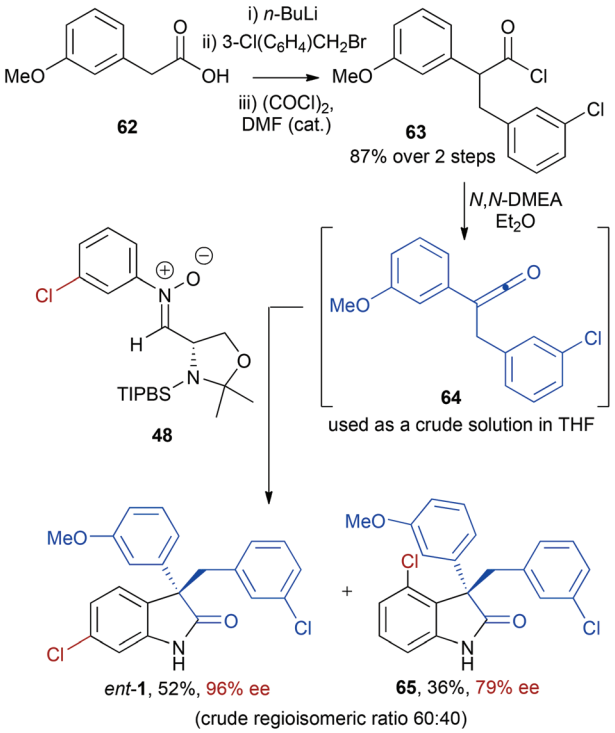

Scheme 4 Application of this methodology to the synthesis of Roche anti-cancer agent *ent*-**1**, and novel analogue **65**.

and 96% ee, whilst the novel regioisomer **65** was isolated in 36% yield and 79% ee.

Conclusions

In summary, the optimization of the asymmetric hetero-Claisen approach to oxindoles has been demonstrated. By variation of the chiral nitrone structure, *N*-TIPBS nitrone **20** was identified as an excellent transmitter of chiral information in reaction with a variety of alkylarylketenes (>15 examples). A range of substituted aryl *N*-TIPBS nitrones was also prepared and used in a survey of the regioselectivity of this transformation (8 examples). These synthetic studies are consistent with the previous computational examination of this reaction system, and the proposed pericyclic cascade mechanism accounts for the observed levels of enantioselectivity.

Further computational investigation revealed that the traditionally invoked mechanistic rationale for this process is energetically improbable under the reaction conditions, and instead results in a dissociative, non-productive fragmentation event. In contrast, the proposed 3 + 2, [3,3]-cascade mechanism is found to be a facile, energetically downhill process, and is substantiated by the isolation of oxazolidinone **59**. As a demonstration of synthetic utility, this methodology was used in a concise, asymmetric preparation of Roche p53 inhibitor *ent*-**1** in 96% ee, along with novel regioisomer **65**. Current efforts within our laboratory are focused on application of this asymmetric methodology in complex molecule synthesis.

Acknowledgements

We thank the Royal Society for a URF (ADS), Cancer Research UK (ER), the Leverhulme Trust (ND) and EPSRC (KBL) for funding. We are also grateful to the National Science Foundation (USA) for financial support of the research at UCLA (KNH). We thank J. Douglas and S. M. Leckie for preparation of previously reported ketenes and Andrew Thomas (Roche) for data related to oxindole **1**. We also thank the EPSRC National Mass Spectrometry Service Centre (Swansea).

We also thank the UCLA Institute for Digital Research and Education (IDRE), the XSEDE resources provided by the XSEDE Science Gateways Program (TG-CHE040013N) of the National Science Foundation (USA), and TUBITAK ULAKBIM High Performance and Grid Computing Center (TRUBA, Turkey) for generous computer time.

Notes and references

1 (*a*) K. C. Nicolaou, D. J. Edmonds and P. G. Bulger, *Angew. Chem., Int. Ed.*, 2006, **45**, 7134–7186, and references therein; (*b*) K. C. Nicolaou and J. S. Chen, *Chem. Soc. Rev.*, 2009, **38**, 2993–3009; (*c*) A. Padwa, *Chem. Soc. Rev.*, 2009, **38**, 3072–3081; (*d*) B. B. Toure and D. G. Hall, *Chem. Rev.*, 2009, **109**, 4439–4486; (*e*) E. A. Anderson, *Org. Biomol. Chem.*, 2011, **9**, 3997–4006.

2 (*a*) K. N. Houk, J. Gonzalez and Y. Li, *Acc. Chem. Res.*, 1995, **28**, 81–90; (*b*) P. H.-Y. Cheong, C. Legault, J. M. Um, N. Çelebi-Ölçüm and K. N. Houk, *Chem. Rev.*, 2011, **111**, 5042–5137. For a related pericyclic cascade approach to this manuscript that utilizes a nitrone 3 + 2 cycloaddition followed by [3,3]-sigmatropic rearrangement see: D.-L. Mo, D. J. Wink and L. L. Andersen, *Chem. – Eur. J.*, 2014, **20**, 13217–13225.

3 (*a*) G. I. Elliott, J. Velicky, H. Ishikawa, Y. Li and D. L. Boger, *Angew. Chem., Int. Ed.*, 2006, **45**, 620–622; (*b*) J. Poulin, C. M. Grise-Bard and L. Barriault, *Chem. Soc. Rev.*, 2009, **38**, 3092–3101.

4 For reviews, see: (*a*) C. Marti and E. M. Carreira, *Eur. J. Org. Chem.*, 2003, 2209–2219; (*b*) C. V. Galliford and K. A. Scheidt, *Angew. Chem., Int. Ed.*, 2007, **46**, 8748–8758.

5 M. K. Christensen, K. D. Erichsen, C. Trojel-Hansen, J. Tjørnelund, S. J. Nielsen, K. Frydenvang, T. N. Johansen, B. Nielsen, M. Sehested, P. B. Jensen, M. Ikaunieks, A. Zaichenko, E. Loza, I. Kalvinsh and F. Björkling, *J. Med. Chem.*, 2010, **53**, 7140–7145.

6 T. D. Bagul, G. Lakshmaiah, T. Kawabata and K. Fuji, *Org. Lett.*, 2002, **4**, 249–251.

7 (*a*) L. E. Overman and Y. Shin, *Org. Lett.*, 2007, **9**, 339–341; (*b*) J. E. DeLorbe, S. Y. Jabri, S. M. Mennen, L. E. Overman and F.-L. Zhang, *J. Am. Chem. Soc.*, 2011, **133**, 6549–6552.

8 J. Christoffers and A. Mann, *Angew. Chem., Int. Ed.*, 2001, **40**, 4591–4597.

9 (*a*) B. M. Trost and M. K. Brennan, *Synthesis*, 2009, 3003–3025; (*b*) F. Zhou, Y.-L. Liu and J. Zhou, *Adv. Synth. Catal.*,

2010, **352**, 1381–1407; (*c*) L. M. Repka and S. E. Reisman, *J. Org. Chem.*, 2013, **78**, 12314–12320.
10 P. B. Alper, C. Meyers, D. R. Lerchner, D. R. Siegel and E. M. Carreira, *Angew. Chem., Int. Ed.*, 1999, **38**, 3186–3189.
11 S. Edmonson, S. J. Danishefsky, L. Sepp-Lorenzino and N. Rosen, *J. Am. Chem. Soc.*, 1999, **121**, 2147–2155.
12 R. He, C. Ding and K. Maruoka, *Angew. Chem., Int. Ed.*, 2009, **48**, 4559–4561.
13 (*a*) S. Lee and J. F. Hartwig, *J. Org. Chem.*, 2001, **66**, 3402–3415; (*b*) J. E. M. N. Klein and R. J. K. Taylor, *Eur. J. Org. Chem.*, 2011, 6821–6841.
14 A. B. Douney, K. Hatanaka, J. J. Kodanko, M. Oestreich, L. E. Overman, L. A. Pfeifer and M. M. Weiss, *J. Am. Chem. Soc.*, 2003, **125**, 6261–6271.
15 (*a*) L. E. Overman and M. D. Rosen, *Angew. Chem., Int. Ed.*, 2000, **39**, 4596–4599; (*b*) A. B. Douney and L. E. Overman, *Chem. Rev.*, 2003, **103**, 2945–2964.
16 (*a*) P. E. Kündig and Y.-X. Jia, *Angew. Chem., Int. Ed.*, 2009, **48**, 1636–1639; (*b*) R. J. K. Taylor and A. Perry, *Chem. Commun.*, 2009, 3249–3251.
17 (*a*) B. M. Trost and M. Osipov, *Angew. Chem., Int. Ed.*, 2013, **52**, 9176–9181; (*b*) B. M. Trost and M. K. Brennan, *Org. Lett.*, 2006, **8**, 2027–2030.
18 I. D. Hills and G. C. Fu, *Angew. Chem., Int. Ed.*, 2003, **42**, 3921–3924.
19 G. S. Singh and Z. Y. Desta, *Chem. Rev.*, 2012, **112**, 6104–6155.
20 (*a*) K. Zheng, C. Yin, X. Lin, L. Lin and X. Feng, *Angew. Chem., Int. Ed.*, 2011, **50**, 2573–2577; (*b*) B. Tan, G. Hernandez-Torres and C. F. Barbas III, *J. Am. Chem. Soc.*, 2011, **133**, 12354–12357.
21 (*a*) G. Lakshmaiah, T. Kawabata, M. Shang and K. Fuji, *J. Org. Chem.*, 1999, **64**, 1699–1704; (*b*) S. Ma, X. Han, S. Krishnan, S. C. Virgil and B. M. Stoltz, *Angew. Chem., Int. Ed.*, 2009, **48**, 8037–8041.
22 H. Staudinger and G. Miescher, *Helv. Chim. Acta*, 1919, **2**, 554–582.
23 C. H. Hassall and A. E. Lippman, *J. Chem. Soc.*, 1953, 1059–1063.
24 M. Hafiz and G. A. Taylor, *J. Chem. Soc., Perkin Trans. 1*, 1980, 1700–1705.
25 N. Duguet, A. M. Z. Slawin and A. D. Smith, *Org. Lett.*, 2009, **11**, 3858–3861.
26 E. Richmond, N. Duguet, A. M. Z. Slawin, T. Lebl and A. D. Smith, *Org. Lett.*, 2012, **14**, 2762–2765.
27 N. Çelebi-Ölçüm, Y.-h. Lam, E. Richmond, K. B. Ling, A. D. Smith and K. N. Houk, *Angew. Chem., Int. Ed.*, 2011, **50**, 11478–11482.
28 R. W. Hoffmann, *Chem. Rev.*, 1989, **89**, 1841–1860.
29 In our previous studies (ref. 26), the corresponding aldehyde has been isolated from a crude reaction mixture and retreated with PhNHOH to regenerate TIPBS nitrone **20**. The nitrone has then been shown to be an effective chiral auxiliary in a second cycle of asymmetric oxindole synthesis.
30 A brief solvent and temperature screen was undertaken (see ESI† for details). The use of THF as solvent at a reaction temperature of −78 °C remained optimal for both yield and enantioselectivity of the product oxindole.
31 The obtained silyl-nitrones were found to hydrolyze on attempted purification by column chromatography, and were not amenable to storage. Consequently, these nitrones were prepared and used immediately as crude residues and only limited characterization data was obtained. Their instability, however, rendered them impractical as potential nitrone chiral auxiliaries.
32 CCDC 1029035 contains the supplementary crystallographic data for **20**.
33 M. J. Frisch, *et al.*, *Gaussian 09, revision A.2*, Gaussian, Inc., Wallingford, CT, 2009. See ESI† for the full citation.
34 H. R. Seikaly and T. T. Tidwell, *Tetrahedron*, 1986, **42**, 2587–2613.
35 C. E. Cannizzaro, T. Strassner and K. N. Houk, *J. Am. Chem. Soc.*, 2001, **123**, 2668–2669.
36 π-π interactions displayed in the X-ray structure of nitrone **20** suggest the importance of dispersion interactions in determining the selectivity at the cycloaddition step. Optimizations using dispersion corrected density functional theory gave similar geometries and relative energies; the results of calculations at the B3LYP-D3/6-311+G(d,p)//B3LYP-D/6-31G(d) level are given in the ESI.†
37 For all reactions described herein, racemic oxindole samples were obtained from reaction of the requisite achiral diarylnitrone and alkylarylketene (see ESI† for Experimental details). For the enantioenriched oxindoles, the absolute configuration is assigned by analogy to that determined by derivatization in our earlier publication (ref. 25).
38 J. E. DeLorbe, D. Horne, R. Jove, S. M. Mennen, S. Nam, F.-L. Zhang and L. E. Overman, *J. Am. Chem. Soc.*, 2013, **135**, 4117–4128.
39 After fourteen days, an ee value of 30% was obtained when the HPLC sample of oxindole **37** was reanalyzed.
40 N. Çelebi-Ölçüm, B. W. Boal, A. D. Huters, N. K. Garg and K. N. Houk, *J. Am. Chem. Soc.*, 2011, **133**, 5752–5755.
41 Stokes and Taylor have described the isolation of a very similar lactone species using the same xylylnitrone starting material: D. P. Stokes and G. A. Taylor, *J. Chem. Soc. C*, 1971, 2334–2336. The relative configuration within **55** was confirmed by single crystal X-ray diffraction. CCDC 1029036 contains the supplementary crystallographic data for **55**.
42 The relative configuration within **59** was confirmed by single crystal X-ray diffraction. CCDC 1029037 contains the supplementary crystallographic data for **59**.
43 The generation of oxazolidinones in reactions of symmetric ketenes and nitrones has been previously observed and investigated; for selected examples see: R. N. Pratt, D. P. Stokes and G. A. Taylor, *J. Chem. Soc., Perkin Trans. 1*, 1975, 498–503; M. A. Abou-Gharbia and M. M. Jouillie, *J. Org. Chem.*, 1979, **44**, 2961–2966. Through an ^{17}O label-

ing study, Evans and Taylor provided experimental evidence for the proposed 3 + 2 cycloaddition/[1,3]-rearrangement pathway for the formation of oxazolidinones from diarylnitrones and ketenes. The possibility of α-lactone formation in this transformation via oxygen atom transfer to ketenes was also probed. However, a subsequent competing deoxygenation-recombination mechanism involving the addition of α-lactones to nitriles and imines was concluded to be an unlikely mechanistic pathway for this transformation. For further details, see: A. R. Evans and G. A. Taylor, *J. Chem. Soc., Perkin Trans. 1*, 1987, 567–569.

44 p53 is a tumour suppressor protein that is lost or suppressed in the majority of cancer cells. Inhibition of p53 has been shown to have two main therapeutic applications: in sensitizing cancer cells to other forms of chemotherapy and in protecting healthy non-cancerous cells from side effects associated with chemotherapy. For further details, see: A. V. Gudkov and E. A. Komarova, *Biochem. Biophys. Res. Commun.*, 2005, **331**, 726–736.

45 Using the L-serine derived chiral nitrone, the furnished oxindole is the enantiomer of the reported Roche compound. The absolute configuration of **1** prepared in this manuscript was assigned by HPLC analysis by analogy to ref. 46. Please see ESI† for further information.

46 D. Katayev and E. P. Kündig, *Helv. Chim. Acta*, 2012, **95**, 2287–2295.

47 K. C. Luk, S. S. So, J. Zhang and Z. Zhang and F. Hoffmann-La Roche, *AG patent*, WO2006/136606, 2006.

48 J. Guo, S. Dong, Y. Zhang, Y. Kuang, X. Liu, L. Lin and X. Feng, *Angew. Chem., Int. Ed.*, 2013, **52**, 10245–10249.